Analytical Investigation of Two Benchmark Resource Allocation Algorithms for LTE-V2V

Alessandro Bazzi*, *Senior Member, IEEE,* Alberto Zanella, *Senior Member, IEEE,*
Giammarco Cecchini, *Student Member, IEEE,* Barbara M. Masini, *Member, IEEE*

Abstract—**Short-range wireless technologies will enable vehicles to communicate and coordinate their actions, thus improving people's safety and traffic efficiency. Whereas IEEE 802.11p (and related standards) had been the only practical solution for years, in 2016 a new option was introduced with Release 14 of long term evolution (LTE), which includes new features to enable direct vehicle-to-vehicle (V2V) communications. LTE-V2V promises a more efficient use of the channel compared to IEEE 802.11p thanks to an improved PHY layer and the use of orthogonal resources at the MAC layer. In LTE-V2V, a key role is played by the resource allocation algorithm and increasing efforts are being made to design new solutions to optimize the spatial reuse.In this context, an important aspect still little studied, is therefore that of identifying references that allow: 1) to have a perception of the space in which the resource allocation algorithms move; and 2) to verify the performance of new proposals. In this work, we focus on a highway scenario and identify two algorithms to be used as a minimum and maximum reference in terms of the packet reception probability (PRP). The PRP is derived as a function of various parameters that describe the scenario and settings, from the application to the physical layer. Results, obtained both in a simplified Poisson point process scenario and with realistic traffic traces, show that the PRP varies considerably with different algorithms and that there is room for the improvement of current solutions.**

Index Terms—**Connected vehicles; Cellular-V2V; LTE-V2V; Cooperative awareness; Resource allocation.**

I. INTRODUCTION

Connected and automated vehicles promise to change people's lives over the next few years, with increased safety, more efficient traffic management and new services for drivers and passengers. As a complement to automation, the use of short-range wireless communications will improve awareness of the surrounding environment and allow cooperation between vehicles on the move and during maneuvers. At the base of most applications, particularly in terms of safety, there are broadcast messages, hereafter referred as cooperative awareness messages (CAMs),[1] used by each vehicle to inform neighbours of their position, direction, speed and so on.

Until late 2016, the main set of standards designed for short-range vehicular communications were the American wireless access in vehicular environment (WAVE) and the European counterpart cooperative intelligent transport systems (C-ITS)/ITS-G5, both based on IEEE 802.11p at the physical

*Corresponding author.

Alessandro Bazzi, Alberto Zanella, Giammarco Cecchini, and Barbara M. Masini are with CNR, IEIIT, Italy (e-mail: `name.surname@cnr.it`).

[1]Such messages are called CAMs in European standardization [1] and correspond to a subclass of the basic safety messages (BSMs) in the American specifications [2].

(PHY) and medium access control (MAC) layers. At that time, 3GPP included in Release 14 of long term evolution (LTE) the so-called LTE-vehicle-to-anything (LTE-V2X) or, more generally, cellular-V2X (C-V2X) to allow direct short-range communications between vehicles and other devices on the road. In particular, the subset represented by the communication between vehicles takes the name of LTE-vehicle-to-vehicle (LTE-V2V). LTE-V2V promises broader coverage and more efficient use of wireless resources than IEEE 802.11p [3]–[5]. The longer range is possible thanks to the improved channel coding and the possible partial use of the bandwidth (less noise at the receiver), while the greater efficiency is a consequence of the MAC layer characterized by orthogonal resources.

More specifically, LTE-V2V is based on an organization of time and frequency domains in orthogonal resources; nodes that use different combinations cause negligible reciprocal interference. One of the main problems is therefore the design of an efficient resource allocation scheme that guarantees a different assignment to the nodes located close to each other. Clearly, the specific algorithm plays a key role in system performance.

Very recently, a number of works concerning the resource allocation algorithms for LTE-V2V have been published both by assuming network support [6]–[9] and a distributed approach [10]–[14]. Obviously, every time a new algorithm has been proposed, an improvement has been shown with respect to some reference; however: 1) there is no agreement on the references to be used; and 2) a discussion about the distance from an optimal allocation is not present. Furthermore, the packet reception probability (PRP) is normally estimated by means of simulations and no analytical expressions are provided.

To deal with this gap, in this paper we focus on CAM transmissions in a highway scenario and identify two algorithms to be used as references. For both of them, we derive the PRP analytically. The first reference corresponds to a random allocation, in which each assignment is performed without any knowledge of the resources occupied by the other nodes; this algorithm represents a pessimistic solution, to be used as an inferior benchmark. The second exploits the exact position of all the vehicles and assigns resources in order, thus maximizing the average distance between the interfering nodes (as better discussed later); this algorithm represents an optimistic solution, to be used as a superior benchmark.

The contribution of the paper is based on the following five steps.

1) We formalize the PRP evaluation in LTE-V2V in a highway scenario, formulating the problem based on the source-destination distance;

2) We focus on a random assignment as a pessimistic reference, indicated in the further as *basic reference*, and derive the relative PRP;

3) We indicate the scheme that maximizes the average distance between the interfering nodes, allocating the resources following the order of the node positions, as an optimistic benchmark, denoted as *maximum reuse reference*, and derive the relative PRP;

4) We provide examples of results to demonstrate the correctness of the analysis for two different highway scenarios: in the first one, the positions of the vehicles are modelled as a homogeneous 1-D Poisson point process (PPP); in the second one, realistic traffic traces are adopted;

5) We also show example results that compare the two benchmarks with algorithms based on specifications and literature.

The rest of the paper is organized as follows. Section II gives a brief overview of LTE-V2V and related work. In Section III, the notation, the scenario and the assumptions are detailed and the problem is formally defined. In Section IV, the two reference algorithms are discussed in detail and the PRP is derived. The numerical results that demonstrate the validity of the analysis and show some relevant examples are provided in Section V. Finally, our conclusions and a discussion of directions for future improvements are provided in Section VI.

II. LTE-V2V AND RELATED WORK

1) LTE-V2V physical and MAC layers: The first C-V2X specifications are included in Release 14, frozen in June 2017 [3], [4]. They are based on device-to-device (D2D) communication, defined as part of the proximity services (ProSe) since Release 12. Direct V2V communications, also referred to as *sidelink*, use single carrier-frequency division multiple access (SC-FDMA) at the PHY and MAC layers (same as the LTE uplink). In the frequency domain, the available bandwidth is separated into groups of orthogonal sub-carriers (12 contiguous sub-carriers, spaced 15 kHz apart from each other). In the time domain, the signal is separated into 10 ms frames, which are in turn subdivided into 10 subframes of 1 ms. A subframe normally accommodates hosts 14 orthogonal frequency division multiplexing (OFDM) symbols, of which nine contain data, four are used for channel estimation and synchronization, and the last one is not used to allow timing adjustments and Tx-Rx switching.

The minimum unit for the allocation of resources is the pair of resource blocks (RBs), corresponding to a group of sub-carriers in the frequency domain and a subframe in the time domain. Depending on the adopted modulation and coding scheme (MCS), the RB pair carries a variable number of data bits, as described for example in [17]; it follows that the number of RBs needed to allocate a message depends both on the size of the packet and on the MCS adopted.

In LTE-V2X, sidelink resource allocation can be performed using one of the following two approaches, defined Mode 3 and Mode 4. In Mode 3, the allocation is performed by a central resource management entity that communicates decisions to individual devices. This mode is only possible if the devices are under coverage of the cellular network. In Mode 4, the allocation is performed autonomously by each vehicle and is therefore completely distributed.

Since the main service is the transmission of CAMs, which is by nature periodic with messages of constant size, a mechanism called semi-persistent scheduling (SPS) is used; the SPS implies that the same resources are allocated periodically for a certain time, minimizing the load caused by the signaling. While a specific algorithm is defined in Release 14 for Mode 4 [18], [19], the algorithm to be used in Mode 3 is left to the network operator.

2) Related work: Several papers have recently addressed the comparison between LTE-V2V and IEEE 802.11p. When and how much LTE-V2V outperforms IEEE 802.11p, it is still under discussion. While some works, such as [20], [21], show significant improvements with the new technology, others observe that it also depends on the specific scenario and settings. For example, both [5] and [10] show that under high load conditions (heavy traffic and/or frequent messages), specific IEEE 802.11p settings may result in a higher PRP.

The impact of the resource allocation algorithm on system performance is indeed so relevant that several studies have recently focused on it, even in the absence of a comparison with IEEE 802.11p. While the first works (such as [22]–[24]) were mainly focused on the underlay scenario, where the same resources can be shared by both V2I and V2V connections, it is now assumed that specific resources will be reserved for V2V communications and attention has been moved more to the spatial reuse of resources.

Examples focused on controlled allocations (Mode 3) are presented in [6]–[9]. In [6], the authors propose an optimized allocation method based on the continuous transmission of the channel state information (CSI) (criticized by some works as not feasible in vehicular scenarios [22]). In [7], the vehicles are clustered and then algorithms based on graph theory are applied to minimize allocation collisions. In [8], the allocation is performed based on a pre-defined reuse distance and vehicle location. In [9], again taking advantage of the position of the nodes, a graph colouring methodology is adopted to correctly select the resource that each vehicle should use based on the assignment of its neighbours.

Autonomous allocations (Mode 4) are investigated in [10]–[14]. While the algorithm specified by 3GPP [18], [19] is addressed in [10], the others focus on new approaches. In both [11] and [12], resources are grouped into sub-pools that are associated with vehicles based on their direction and/or position on the road, thus reducing the risk of collisions due to allocations performed by terminals hidden to each other (mainly because of the distance in the highway scenarios and of the buildings in the urban areas). In [13], the adoption of maps of the resources sent within the CAMs is proposed. In [14], the performance of autonomous selection algorithms is improved by piggybacking information about reservations with the data packets.

The main aspects of the cited papers dealing with resource

TABLE I
RELATED WORK DEALING WITH RESOURCE ALLOCATION IN LTE-V2V.

Reference	LTE Release	Algorithm proposed	Evaluation Tool	Benchmark(s)
Zhang et al. [6]	Before Release 14	Controlled algorithm, based on CSI	Not specified simulator	i) A modified algorithm from the literature and ii) random allocation with check of the SINR
Abanto-Leon et al. [7]	Release 14	Controlled algorithm based on clustering and graph-theory	Not specified simulator	Exhaustive search
Cecchini et al. [8]	Release 14	Controlled algorithm, based on reuse distance	LTEV2Vsim [15]	No benchmark
Hu et al. [9]	Before release 14	Controlled algorithm, based on graph coloring	Not specified simulator	An ideal scheme, without interference
Molina-Menegosa et al. [10]	Beyond Release 14	Autonomous, modified from 3GPP	Veins [16]	Standard 3GPP autonomous algorithm
Yang et al. [11]	Before Release 14	Autonomous, based on positions	Not specified simulator	Random allocation
Kim et al. [12]	Before Release 14	Autonomous, based on positions	Not specified simulator	Random allocation
Cecchini et al. [13]	Beyond Release 14	Autonomous, with observed occupations piggybacked in data packets	LTEV2Vsim [15]	Two algorithms from the literature
He et al. [14]	Beyond Release 14	Autonomous, with reservations piggybacked in data packets	Ad-hoc simulator	Random allocation and basic enhancements

allocations are also summarized in Table I. In all cases, the results are compared with simpler solutions and it is not possible to understand how much the obtained performance is far from that of an optimal allocation. Furthermore, the results are always obtained by simulation.

Differently, in this work we derive the PRP for a basic and a maximum reuse allocation, with the aim to provide reference indications for the evaluation of new algorithms.

III. SYSTEM MODEL

In this Section, the notation, the scenario, and the assumptions adopted are first detailed, followed by the formulation of the problem.

A. Notation

Throughout the paper, $\mathbb{P}\{\mathcal{A}\}$ and $\mu_X \triangleq \mathbb{E}_X\{\cdot\}$ indicate the probability of the event $\mathcal{A}$, and the expectation with respect to the random variable (r.v.) X, respectively. The functions $f_X(x)$, $F_X(x)$, and $\bar{F}_X(x)$ respectively indicate the probability density function (PDF), the cumulative distribution function (CDF) and the complementary cumulative distribution function (CCDF) ($\mathbb{P}\{X > x\}$) of the r.v. X. Finally, $g'(x) \triangleq dg(x)/dx$ is the derivative of the function g with respect to the variable x.

B. Scenario and assumptions

1) Scenario: In this work, we assume a highway segment with variable traffic conditions, approximated as a 1-D scenario with vehicles distributed according to Poisson, i.e., the vehicle positions follow a homogeneous PPP. It has been shown that this approximation is in good agreement with the real distributions (refer, for example to [25], [26]). The validity of our results is anyway discussed in Section V also with reference to a realistic highway scenario. In the following, x_n indicates the coordinate of vehicle n; without loss of generality, the vehicles in the scenario are numbered in such a way that $x_i < x_j$ if $i < j$. An example of a 2-D scenario with its 1-D representation is provided in Figs. 1(a) and 1(b).

2) Resources: Each vehicle is equipped with an on board unit (OBU) that periodically generates CAMs at a certain frequency f_{CAM}, i.e., with a given repetition interval $T_{\mathrm{CAM}} = 1/f_{\mathrm{CAM}}$. CAMs are all of B_{CAM} bytes. The allocation of a CAM requires the reservation of a group of contiguous RBs (as calculated for example in [17]). Given the periodic nature of packet generation and the fixed size of the messages, during each T_{CAM} it is possible to assign a fixed maximum number of CAMs using a deterministic number of groups of RBs. Such groups are hereafter denoted as CAM resources (CAM-Rs) and the number of CAM-Rs per T_{CAM} is denoted as R. Each message is transmitted in one of the R available CAM-Rs and any two devices interfere with each other if and only if they use the same CAM-R.

Given the use of SC-OFDMA, R corresponds to a grid of R_{f} resources in the frequency domain and R_{t} resources in the time domain (i.e., $R = R_{\mathrm{f}} \cdot R_{\mathrm{t}}$). As for time and frequency domains, resources are ordered so that the generic resource $r^* \in \{1, R\}$ occupies in the time domain the slot $r_{\mathrm{t}}^* = r^* \bmod R_{\mathrm{t}}$ and in the frequency domain the portion $r_{\mathrm{f}}^* = \lceil \frac{r^*}{R_{\mathrm{t}}} \rceil$ (i.e., $r^* = (r_{\mathrm{f}}^* - 1) \cdot R_{\mathrm{t}} + r_{\mathrm{t}}^*$). This means, in particular, that two generic resources r_a and r_b are transmitted in the same time interval if $|r_a - r_b|$ is a multiple of R_{t}.

3) Propagation: The signal attenuation due to propagation is modelled as

$$L(\delta) = \frac{L_0 \cdot \delta^\beta}{\upsilon} \qquad (1)$$

where L_0 is the average path loss at the reference distance of 1 m, δ is the distance between the transmitter and the receiver, β is the path loss exponent, and υ is a random variable that takes into account the channel variability, assumed constant during the transmission of a CAM.

Consider a generic transmitter, a generic receiver at distance δ, and the set of all interferers $\mathcal{N}_{\mathrm{int}}$ (depending on the allocation algorithm). Each interferer $i \in \mathcal{N}_{\mathrm{int}}$ is at a distance $\delta_{\mathrm{int}}^{(i)}$ from the receiver and with an independent channel variability represented by $\upsilon^{(i)}$. All signals are transmitted with the same power P_{t}. The signal to noise and interference ratio (SINR) at the receiver is calculated as

$$\gamma = \frac{P_{\mathrm{r}}}{P_{\mathrm{n}} + I_{\mathrm{tot}}} = \frac{\frac{P_{\mathrm{t}} \cdot G_{\mathrm{t}} \cdot G_{\mathrm{r}} \cdot \upsilon}{L_0 \cdot \delta^\beta}}{P_{\mathrm{n}} + \sum_{i \in \mathcal{N}_{\mathrm{int}}} \frac{P_{\mathrm{t}} \cdot G_{\mathrm{t}} \cdot G_{\mathrm{r}} \cdot \upsilon^{(i)}}{L_0 \cdot \delta_{\mathrm{int}}^{(i)\,\beta}}} \qquad (2)$$

(a) Example 2-D scenario.

(b) 1-D representation.

(c) Example of random resource allocation (RR).

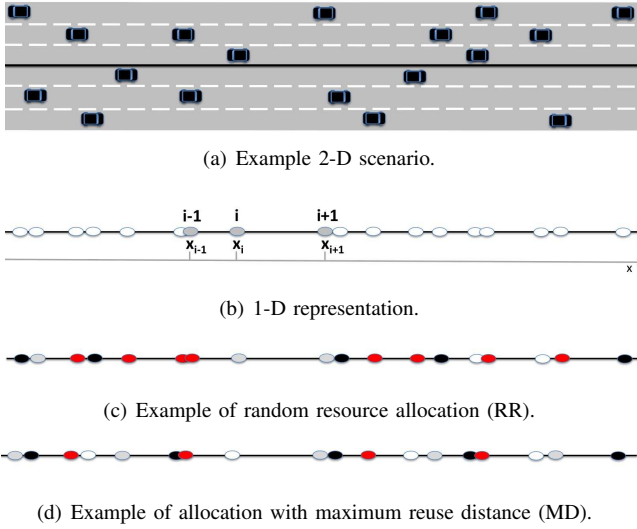(d) Example of allocation with maximum reuse distance (MD).

Fig. 1. Example 2-D scenario, 1-D representation, and example allocations. Allocations are shown assuming $R = 4$, with different colors representing orthogonal resources.

where G_t is the antenna gain at the transmitter, G_r is the antenna gain at the receiver, $P_r = \frac{P_t \cdot G_t \cdot G_r \cdot v}{L_0 \cdot \delta^\beta}$ is the power received from the desired transmitter, P_n is the noise power, and $I_{tot} = \sum_{i \in \mathcal{N}_{int}} \frac{P_t \cdot G_t \cdot G_r \cdot v^{(i)}}{L_0 \cdot \delta_{int}^{(i)\,\beta}}$ is the total interference power.

It is assumed that a message is correctly decoded if γ is greater than a minimum threshold γ_m (as for example in [24]–[28]).

4) Half duplexing: Since the radios of the LTE-V2V devices are half duplex (HD), a node is not able to decode the message in the same subframe that it is using for transmissions. To take this into account, we define the probability of loss due to HD as P_{HD}.

C. Problem formulation

Throughout this paper, the following definitions apply.

- *Source-to-destination distance*, d_{sd}: it is the physical distance between the generic source and the generic destination;
- *PRP*, P_{RP}: it is the probability that a vehicle at a given distance from the source correctly receives and decodes a message; based on the previous definition of correct decoding and taking into account the HD problem, it is

$$P_{RP} = (1 - P_{HD}) \cdot \mathbb{P}\{\gamma > \gamma_m\} . \quad (3)$$

The purpose of this work is to derive P_{RP} as a function of d_{sd}, with the specified settings. All CAMs are considered of the same importance for all receivers, which is a common assumption. In any case, providing results based on the distance between source and destination allows us to differentiate the performance based on how close the vehicles are communicating. It is intuitive, in fact, that the relevance of the information is different if vehicles are close or far from each other; this consideration is also reflected in the requirements for V2V applications, which often include a maximum communication distance [29], [30].

IV. BENCHMARK RESOURCE ALLOCATION ALGORITHMS AND PACKET RECEPTION PROBABILITY EVALUATION

In this Section, the two reference allocations are detailed and the corresponding PRP is calculated, preceded by a discussion on the approach adopted and on the common expressions.

A. Common calculations

The model expressed by (2) includes independent random variables to describe the channel of the useful signal and that of each interfering signal; this makes the conventional mathematical methods not applicable to obtain the desired distribution. To simplify the problem, let us assume that the variability of the channel of the interferers is negligible, i.e. we assume $v^i = 1, \ \forall i \in [1, n_{int}]$. Please note that this approximation is applied only to the analysis and not to the simulations used to validate the model. We also define the received power without the channel variability as $\widetilde{P}_r \triangleq \frac{P_t \cdot G_t \cdot G_r}{L_0 \cdot \delta^\beta}$ and the maximum acceptable interference level for a given v as

$$I_{max}(v) \triangleq \frac{P_r(v)}{\gamma_m} - P_n = \frac{\widetilde{P}_r \cdot v}{\gamma_m} - P_n . \quad (4)$$

Moreover, we denote as $P_{RP}^*(v)$ the probability of correctly decoding a packet, ignoring the problem of the HD and given a specific value of v. According to (2), (4), and the definition of PRP, it follows

$$P_{RP}^*(v) = \mathbb{P}\left\{ I_{tot} < \frac{P_r(v)}{\gamma_m} - P_n \right\}$$
$$= \mathbb{P}\{I_{tot} < I_{max}(v)\} = F_{I_{tot}}(I_{max}(v)) . \quad (5)$$

Finally, since losses due to half duplexing and incorrect decoding are independent of each other, it is

$$P_{RP} = (1 - P_{HD}) \cdot \int_{-\infty}^{\infty} P_{RP}^*(v) \mathbb{P}(v) dv$$
$$= (1 - P_{HD}) \cdot \int_{-\infty}^{\infty} F_{I_{tot}}(I_{max}(v)) \mathbb{P}(v) dv$$
$$= (1 - P_{HD}) \cdot \int_{-\infty}^{\infty} F_{I_{tot}}(\frac{\widetilde{P}_r \cdot v}{\gamma_m} - P_n) \mathbb{P}(v) dv. \quad (6)$$

As a consequence, for any given distribution of the channel variability $\mathbb{P}(v)$, the solution to the problem defined in Section III-C is obtained once the value of P_{HD} and the expressions of $F_{I_{tot}}(y)$ are derived. Being y interference, it is $y \geq 0$; this assumption is left implicit in the following.

B. Random resource allocation (RR)

Algorithm and motivation. We denote as random resource allocation (RR) the selection of resources carried out randomly with uniform distribution. Formally, the CAM-R allocated to node n is

$$r_n = \text{randint}\{1, R\} \quad (7)$$

where randint$\{a, b\}$ corresponds to a uniformly random selection of an integer between a and b. A new selection is performed in each beacon interval. An example of RR is shown in Fig. 1(c), with $R = 4$. Among all the possible

allocations, RR represents a useful reference, since it does not exploit any parameter or knowledge, except for R. If another algorithm performs worse or even slightly better, it is more convenient to replace it with RR to reduce memory occupancy and computational load.

Maximum interference calculation. Since the nodes are positioned according to a 1-D homogeneous PPP and the allocation of resources is completely random, we can apply the Marking Theorem [31] to demonstrate that the set of nodes that adopt a specific resource still follows a 1-D homogeneous PPP. As a consequence, the interfering nodes still follow a 1-D PPP with density $\rho_{\mathrm{RR}} = \rho/R$ and the interference can be calculated using the same approach as [32], [33], leading to the following Proposition.

Proposition 1: The total interference with RR corresponds to a stable distribution with parameters $\mu = 0$, $a = 1/\beta$, $b = 1$, and $c = P_{\mathrm{r0}} \left(2\rho_{\mathrm{RR}} \Gamma \left(\frac{\beta-1}{\beta} \right) \cos \left(\frac{\pi}{2\beta} \right) \right)^{\beta}$, where P_{r0} is defined in (13) and $\Gamma(x) = \int_0^\infty t^{x-1} e^{-t} dt$ is the gamma function.

Proof: The Proof is provided in Appendix A. ∎

Although there is no closed form (with the exception of case $\beta = 2$, detailed in the Lemma that follows), the CDF of the distribution can easily be obtained numerically, for example as proposed in [34].

Lemma 1: If $\beta = 2$, the CDF can be written as

$$F_{I_{\mathrm{tot}}}(y) = \mathrm{erfc}\left(\rho_{\mathrm{RR}} \Gamma(1/2) \sqrt{\frac{P_{\mathrm{r0}}}{y}} \right) . \tag{8}$$

Proof: The Proof is provided in Appendix B. ∎

Probability of the HD issue. Since the selection of the resource is random, the probability that the source and the destination use a resource of the grid that occupies the same time unit is simply

$$P_{\mathrm{HD}} = 1/R_{\mathrm{t}} . \tag{9}$$

C. Allocation with maximum reuse distance (MD)

Algorithm and motivation. We denote as allocation with maximum reuse distance (MD) the allocation obtained by ordering the vehicles based on their position and allocating the resources in cyclic order. Formally, the CAM-R allocated to node n is

$$r_n = n \mod R \tag{10}$$

where $a \mod b$ is used to indicate a modulo b (i.e., the rest of the Euclidean division of a by b). The sorting and allocation process is repeated at each beacon interval. An example of MD is shown in Fig. 1(d), with $R = 4$. MD, inspired by the frequency planning in cellular networks, represents a relevant reference, as it maximizes the average distance between nodes using the same resource, as clarified in the following Proposition.

Proposition 2: In a 1-D PPP, given the number of resources R, the maximum value of the average distance between nodes using the same resource is obtained by sorting the nodes based on their position and then allocating the resources in order, modulo R.

Proof: The Proof is provided in Appendix C. ∎

Please note that, if the channel variability is neglected and taking into account that the interference is monotonically decreasing with distance, the same reasoning can be applied to show that the average interference mutually caused by the nodes is minimized. It should also be observed that the MD algorithm is proposed only as a reference, since its implementation is hardly realistic; in fact, it would require real-time knowledge of the position of all nodes by an entity (e.g., the network) and a continuous communication of the new allocation from the same entity to all nodes.

Maximum interference calculation. With MD the set of interfering nodes is no longer a PPP. In this case, the assessment of the contribution of all the interferers does not appear to be tractable. To obtain a closed-form expression, we approximate the distribution of the interference at the generic destination by considering only the first interferer on the right and the first interferer on the left of the destination node. All other interferers are further away from the destination and are considered negligible. With this approximation, the following Proposition is valid.

Proposition 3: The CDF of the received interference with MD can be approximated by[2]

$$F_{I_{\mathrm{tot}}}(y) \approx K_{\mathrm{MD}} \int_0^y \Gamma\left(R, \rho\left(\xi\left(y-z, -d_{\mathrm{sd}}\right)\right)\right)$$
$$\cdot \left(\xi\left(z, d_{\mathrm{sd}}\right)\right)^{R-1} \xi'(z) e^{-\rho(\xi(z,d_{\mathrm{sd}}))} dz \tag{11}$$

where $K_{\mathrm{MD}} = -\frac{\rho}{(\Gamma(R))^2}$, $\Gamma(s, x) \triangleq \int_x^\infty t^{s-1} e^{-t} dt$ is the upper incomplete gamma function, $\xi(a, b) = \left(\frac{a}{P_{\mathrm{r0}}} \right)^{-\frac{1}{\beta}} + b$, and $\xi'(a) = \frac{d\xi(a,b)}{da} = \left(-\frac{1}{\beta} \right) P_{\mathrm{r0}}^{1/\beta} a^{-\frac{1+\beta}{\beta}}$.

Proof: The proof is provided in Appendix D. ∎

Probability of the HD issue. Since the nodes are sorted and the resources are ordered as specified in Section III-B, the probability that the receiver transmits in the same time interval as the source corresponds to the probability that the number of nodes between them is equal to $(R_{\mathrm{t}} - 1) + k \cdot R_{\mathrm{t}}$, for any integer $k \geq 0$. Given the hypothesis of 1-D PPP, this probability can be derived as

$$P_{\mathrm{HD}} = \sum_{k=0}^\infty \mathbb{P}\{\text{to have } (R_{\mathrm{t}} - 1) + k \cdot R_{\mathrm{t}} \text{ nodes} \in [0, d_{\mathrm{sd}}]\}$$
$$= \sum_{k=0}^\infty \frac{(\rho d_{\mathrm{sd}})^{(R_{\mathrm{t}}-1)+k \cdot R_{\mathrm{t}}}}{((R_{\mathrm{t}}-1)+k \cdot R_{\mathrm{t}})!} e^{-\rho d_{\mathrm{sd}}} . \tag{12}$$

V. Numerical Results

In this Section, example results are shown to validate the models and demonstrate the efficacy of the proposals as references, first in a 1-D PPP scenario and then considering a realistic highway traffic trace.

---

[2]Equation (11) is derived with the following limitations, which are normally acceptable: 1) the probability that there is an interferer between source and destination is negligible; and 2) the useful received power is greater than the minimum acceptable interference. The general solution is also provided in Appendix D.

TABLE II
MAIN SETTINGS.

Parameter (Symbol)	Value
Vehicle density (ρ)	0.1 vehicles/m (*)
Source to destination distance (d_{sd})	120 m (*)
Beacon frequency	10 Hz (*)
Transmitted power (P_{t})	23 dBm
Antenna gain at the transmitter (G_{t})	3 dB
Antenna gain at the receiver (G_{r})	3 dB
Path loss at 1 m (L_0)	20.06 dB
Loss exponent (β)	4
Noise figure	9 dB
Bandwidth	10 MHz
Pairs of RBs per subframe for data	40
MCS	4
Modulation	QPSK
Beacon size (B_{CAM})	300 bytes
RBs per beacon	68
Beacon resources per beacon period (R)	100 (*)
Minimum SINR (γ_{m})	2.8 dB

(*) Value used when not differently specified

Fig. 2. PPP scenario. Packet reception ratio vs. distance.

A. Main settings

The main settings are summarized in Table II. In accordance with 3GPP in [35], we have adopted $B_{\text{CAM}} = 300$ bytes, a bandwidth of 10 MHz, $G_{\text{t}} = G_{\text{r}} = 3$ dB, a noise figure of 9 dB, and the WINNER+ B1 model [36] for propagation, corresponding to $L_0 = 20.06$ dB and $\beta = 4$.[3] To model the channel variability, we assume the presence of log-normal shadowing with a standard deviation of 3 dB, as recommended by 3GPP in [35]; in the simulations, the shadowing is correlated, with decorrelation distance 25 m. A transmission power of $P_{\text{t}} = 23$ dBm is assumed, equal to the maximum transmission power allowed in [37].

MCS 4 is adopted with the following rationale. Assuming as in [5] that 40 RB pairs are available in each LTE subframe for CAM allocation, MCS 4 is the most reliable MCS that does not require more than one subframe to allocate a beacon of $B_{\text{CAM}} = 300$ bytes (each CAM uses 68 RBs). The allocation of a CAM per subframe ($R_{\text{f}} = 1$) leads to a number of CAM-Rs $R = R_{\text{t}}$ and a threshold $\gamma_{\text{m}} = 2.8 \ dB$ (obtained as in [17]). Unless otherwise specified, a beacon frequency of 10 Hz is assumed, which is the most commonly adopted value and corresponds to $R = R_{\text{t}} = 100$ (recalling that a subframe lasts 1 ms).

In addition to RR and MD, the performance of the following allocation algorithms, obtained by simulation, are shown.

- *Centralized with resource reuse (CRR)*: applying the algorithm detailed in [8], the network allocates the resources based on the position of vehicles (which is assumed to be known with a Gaussian error of less than 100 m in 95% of the cases). The algorithm ensures that two nodes are never assigned the same resource if their distance is less than a given value, set here at 200 m; the node is blocked (i.e., no resources are temporarily allocated) if no CAM-R respects this condition;

- *Location-based graph coloring (LGC) algorithm*: applying the algorithm detailed in [9], the network allocates the resources trying to maximize the distance between nodes using the same CAM-R; more specifically, it considers the vehicles in random order and, after allocating a different time-frequency combination to the first R vehicles, allocates to each of the following vehicles, one after the other, the CAM-R that is used farther than its position, exploiting the Euclidean distance; perfect knowledge of positions and a reallocation every T_{CAM} are assumed to maximize its performance;

- *3GPP Autonomous with $p_{keep} = 0$ (M4,$p_{keep} = 0$) and 3GPP Autonomous with $p_{keep} = 0.8$ (M4,$p_{keep} = 0.8$)*: with the 3GPP algorithm, detailed in [10], [18], [19], the resources are allocated autonomously by the nodes, without any contribution from the network. Each node selects the resource randomly in the 20% less interfered CAM-Rs, based on the local channel sensing and limiting the choice to those that the control channel indicates as free or for which the measured interference is below a parametric threshold I_{th} (here assumed -110 dB as in [10]); then, after a period of time randomly selected within a range of 0.5-1.5 s, the node changes allocation with probability $1 - p_{\text{keep}}$, where $p_{\text{keep}} \in [0, 0.8]$ is a parameter which defines the probability of maintaining the same allocation. Since p_{keep} has a significant influence on the performance [38], [39], here we consider both extremes, i.e., $p_{\text{keep}} = 0$ and $p_{\text{keep}} = 0.8$.

All the simulations, shown together with the 95% *t*-test based confidence interval, have been obtained using the LTEV2Vsim open source simulator [15]. We also remark that in all the simulations i) the mobility is reproduced in detail, ii) all the interferers are always considered in the calculation of SINR, iii) all the signals, including those from interferers, are affected by correlated shadowing. This allows to validate the approximations made in the analysis.

---

[3]In principle, the WINNER+ B1 model [36] has a dual-slope, with the given values that are valid for distances larger than about 20 m. However, this distance is very small in the considered scenario. For simplicity, the analysis is therefore approximated as single-slope. In any case, all the simulations were performed using the dual-slope model.
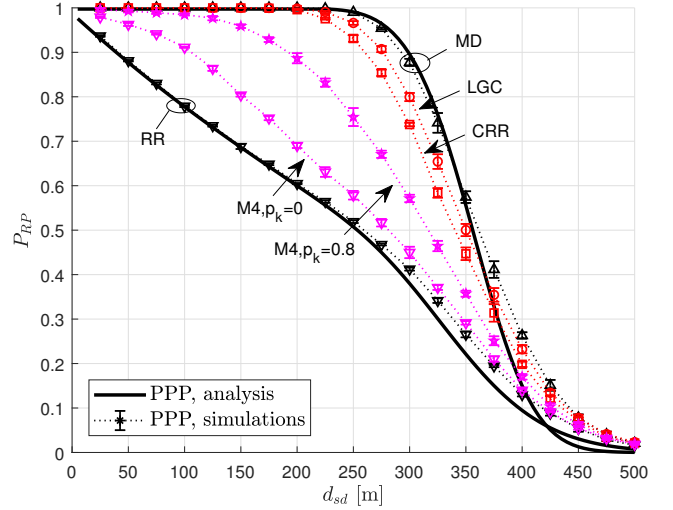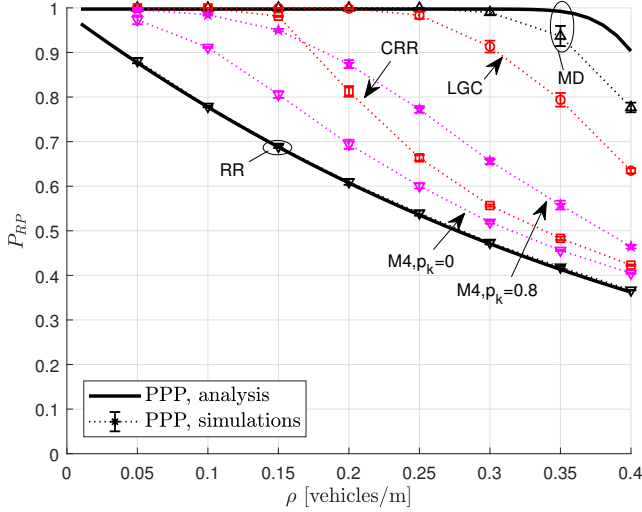
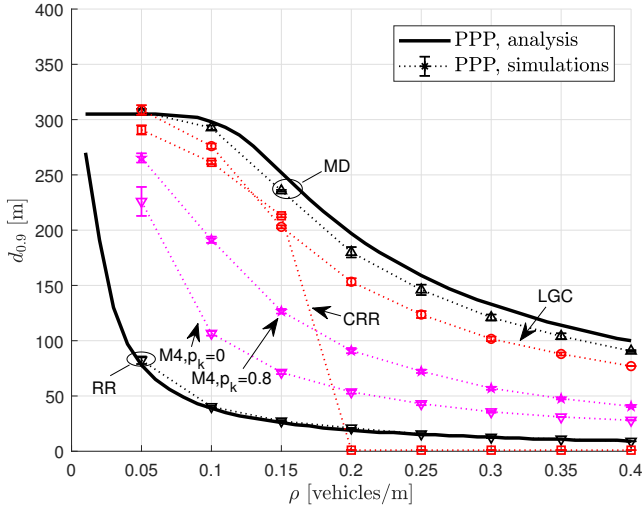Fig. 3. PPP scenario. Packet reception ratio vs. density, with $d_{sd} = 100$ m.

Fig. 4. PPP scenario. Maximum distance allowing $P_{RP} > 0.9$ vs. density.

B. Results in a 1-D PPP scenario

The first set of results assumes that the vehicles are distributed following a 1-D homogeneous PPP. In Fig. 2, P_{RP} is shown varying d_{sd}. Regarding RR and MD, the first observation is that the agreement between simulation and analysis is extremely good.

Focusing on MD, Fig. 2 presents near-threshold behaviour for P_{RP}: it stays close to 1 until $d_{sd} < 300$ m and then drops rapidly to 0. For large values of d_{sd}, other allocations (including RR) may statistically imply the existence of a few nodes that perceive a limited amount of interference, which leads to P_{RP} better than that obtained with MD. However, this effect only occurs when the conditions of link quality are very poor and the value of P_{RP} is unacceptably small.

Another important aspect to highlight observing Fig. 2 is the very high difference between MD and RR, with the former allowing about twice as much P_{RP} in some conditions. This confirms that the specific algorithm used for resource allocation has a significant impact on the performance of LTE-

V2V.

Focusing now on the remaining curves (i.e., CRR, LGC, M4,$p_{keep} = 0$, and M4,$p_{keep} = 0.8$), it is of paramount importance to observe that they all remain between RR and MD: the one providing worse performance (i.e., M4,$p_{keep} = 0$) is preferable to RR and the one with the highest PRP (i.e., LGC) does not reach MD. This confirms that the proposed algorithms can be used as references for the validation of new proposals. Less relevant to the purpose of this paper, but still interesting to note, is that the curves confirm that network controlled algorithms (i.e., CRR and LGC) in most cases lead to higher PRP than autonomous algorithms (i.e., M4,$p_{keep} = 0$ and M4,$p_{keep} = 0.8$).

Similar conclusions can also be drawn from Figs. 3 and 4, which show, as a function of the vehicle density ρ, respectively P_{RP} and $d_{0.9}$. The parameter $d_{0.9}$, in particular, is defined as the maximum distance between source and destination that guarantees $P_{RP} > 0.9$. As a premise, as regards CRR in Fig. 4, note that $d_{0.9}$ falls to zero for $\rho \geq 0.2$; this can be explained by observing that the density is so high that the algorithm blocks more than 10% of the nodes; since the blocked nodes contribute as if the corresponding messages were not received, the target $P_{RP} > 0.9$ can not be reached at any distance. The same reason, leads CRR in Fig. 3 to perform worse than M4,$p_{keep} = 0.8$ for ρ greater than 0.15 vehicles/m. Observing now both figures, the comparison between theoretical benchmarks and simulation confirms the validity of the analysis. In particular, it should be noted that the approximation adopted in MD to consider only the first interferer on both sides has a negligible impact on the overall results. Moreover, also in this case we can observe that RR and MD appear as inferior and superior references for all the other algorithms.

C. Results in a realistic highway scenario

The second set of results compares the benchmark curves with simulations carried out in a realistic highway scenario. More specifically, vehicle positions are obtained from a traffic trace that represents a congested highway with three lanes per direction (details can be found in [40]).[4] There are on average 2015 vehicles distributed over 16 km, corresponding to a density of $\rho = 0.125$ vehicles/m. The benchmark curves are obtained by applying the same density to the analysis.

In Fig. 5, P_{RP} is shown by varying d_{sd}. The results are not generally different from those presented focusing on the 1-D PPP scenario and once again confirm that the two proposed algorithms represent valid references to evaluate the effectiveness of the resource allocation schemes. In addition to what has already been discussed, Fig. 5 allows us to derive the following consideration: although the simulation results have been obtained with a different model (realistic highway traces instead of PPP), the theoretical reference curves are very close to those of the simulations; therefore, the curves obtained can be used not only in an ideal PPP scenario, but also in realistic highway conditions.
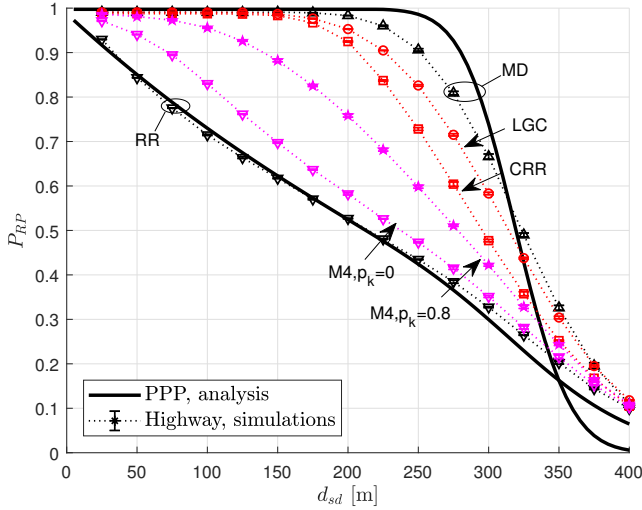
Fig. 5. Highway scenario (the analysis assumes 1-D PPP with the same density). Packet reception ratio vs. distance.
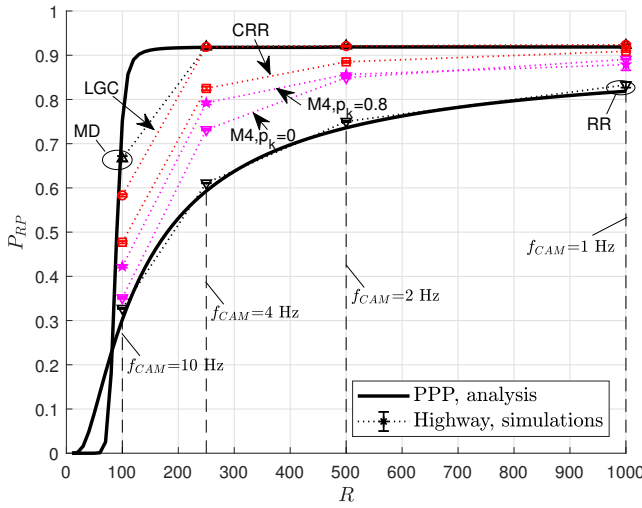

Fig. 6. Highway scenario (the analysis assumes 1-D PPP with the same density). Packet reception ratio vs. number of resources that follows a variable CAM frequency, with $d_{sd} = 300$ m.

Finally, Fig. 6 shows P_{RP} depending on the number of available resources R, or equivalently, as a function of the beacon frequency, f_{CAM} (from 1 to 10 Hz). Besides confirming once again the analysis and the suitability of MD and RR as benchmarks, the figure shows that the impact of the allocation algorithm increases as resources get scarce; therefore, the design of an efficient algorithm becomes more important with an increase of f_{CAM}.

VI. CONCLUSION AND FUTURE WORK

The objective of this article is to define benchmarks that provide a clear reference to quantify the performance of the resource allocation algorithms designed for LTE-V2X. In particular, two algorithms are identified, one as an inferior and the other as a superior reference, and their performance is obtained analytically in terms of packet reception ratio in a highway scenario. The correctness of the analysis has been demonstrated with simulations, which also include aspects that

are simplified in the analysis. Furthermore, the actual usability of these benchmarks has been shown using four allocations taken from the literature, which provide results that remain within the space indicated by the derived curves. Although obtained with a 1-D PPP assumption, it has been shown that the results are valid also in realistic highway scenarios. By providing references to the performance that can be achieved, these benchmarks will be a useful tool to help in the definition and validation of new allocation algorithms.

As further improvements to the proposed analytic framework, we will work to also take into account variable beacon generation rates, given that both ETSI and SAE standards include mechanisms to make cooperative awareness message generation adaptive to channel occupation. In addition, we will extend the investigation to other relevant metrics, such as latency and update delay (distribution of the delay between consecutive updates of a given vehicle).

APPENDIX A: PROOF OF PROPOSITION 1

Let us consider the set of nodes, characterized by the positions x_k, which adopt the same resource r. For the considerations expressed in Section IV-B, this set still belongs to a 1-D homogeneous PPP with density ρ_{RR}. Now, let I_k denote the interference received by the generic node k, at position x_k, provided by a transmitter at position $x = 0$. Defining

$$P_{r0} \triangleq \frac{P_t G_t G_r}{L_0} \qquad (13)$$

the received power at 1 m, it follows that the interference is equal to

$$I_k = \Upsilon(|x_k|) \triangleq P_{r0}|x_k|^{-\beta} \qquad (14)$$

and the interference provided by all the nodes that use the same resource r can be written as

$$I_{tot} = \sum_{k=-\infty}^{\infty} I_i = \sum_{k=-\infty}^{\infty} \Upsilon(|x_k|) . \qquad (15)$$

To obtain the CDF of I_{tot}, we will first evaluate its characteristic function (c.f.). To this aim, let us consider a finite interval $[-a, a]$. First we provide the c.f. for the finite interval and, then, calculate the limit for $a \to \infty$. Since nodes are distributed according to a homogeneous PPP, if $\Phi_{I_{tot}}(\omega)$ is the c.f. of I_{tot}, then [32]

$$\Phi_{I_{tot_a}}(\omega) = e^{\mu_N(\Phi_{I_{i_a}}(\omega)-1)} \qquad (16)$$

where $\Phi_{I_{i_a}}(\omega)$ is the c.f. of interference generated by a generic node in $[-a, a]$ and $\mu_N = 2a\rho_{RR}$ is the expected value of the number of nodes in the interval.

To calculate $\Phi_{I_{i_a}}(\omega)$, recall that the PDF of the distance between a generic interfering node and the receiver located at $x = 0$ is

$$f_{R_a}(\delta) = 1/a, \quad \delta \in [0, a]. \qquad (17)$$

In such case, it is

$$\Phi_{I_{i_a}}(\omega) = \mathbb{E}_{R_a}\left\{e^{j\omega\Upsilon(|x|)}\right\} = \int_0^a f_{R_a}(\delta)e^{j\omega\Upsilon(\delta)}d\delta$$

$$= \frac{1}{a}\int_0^a e^{j\omega\Upsilon(\delta)}d\delta \qquad (18)$$

which becomes, after the change of variable $y = \Upsilon(\delta)$, $\delta = \Upsilon^{-1}(y)$, $d\delta = [\Upsilon^{-1}(y)]' dx$ and an integration by parts

$$
\begin{aligned}
\Phi_{I_{i_a}}(\omega) &= \frac{1}{a} \int_{\Upsilon(0)}^{\Upsilon(a)} e^{j\omega y} [\Upsilon^{-1}(y)]' dy \\
&= \frac{1}{a} \left[\left[\Upsilon^{-1}(y) e^{j\omega y} \right]_{\Upsilon(0)}^{\Upsilon(a)} - j\omega \int_{\Upsilon(0)}^{\Upsilon(a)} \Upsilon^{-1}(y) e^{j\omega y} dy \right] \\
&= \frac{1}{a} \left[a e^{j\omega \Upsilon(a)} - j\omega \int_{\Upsilon(0)}^{\Upsilon(a)} \Upsilon^{-1}(y) e^{j\omega y} dy \right] . \quad (19)
\end{aligned}
$$

By substituting (19) in (16), we get

$$
\begin{aligned}
\Phi_{I_{\text{tot}_a}}(\omega) &= e^{\mu_N (\Phi_{I_{i_a}}(\omega) - 1)} \\
&= e^{2\rho_{\text{RR}} a \left[\frac{1}{a} \left(a e^{j\omega\Upsilon(a)} - j\omega \int_{\Upsilon(0)}^{\Upsilon(a)} \Upsilon^{-1}(y) e^{j\omega y} dy \right) - 1 \right]} \\
&= e^{2\rho_{\text{RR}} a \left[\left(e^{j\omega\Upsilon(a)} - 1 \right) - \frac{j\omega}{a} \int_{\Upsilon(0)}^{\Upsilon(a)} \Upsilon^{-1}(y) e^{j\omega y} dy \right]} \\
&= e^{2\rho_{\text{RR}} a \left(e^{j\omega\Upsilon(a)} - 1 \right)} e^{-j 2\rho_{\text{RR}} \omega \int_{\Upsilon(0)}^{\Upsilon(a)} \Upsilon^{-1}(y) e^{j\omega y} dy}.
\end{aligned}
$$
$$(20)$$

If we now apply the limit for $a \to \infty$, we obtain

$$
\begin{aligned}
\Phi_{I_{\text{tot}}}(\omega) &= \lim_{a \to \infty} \Phi_{I_{\text{tot}_a}}(\omega) \\
&= \lim_{a \to \infty} e^{2\rho_{\text{RR}} a \left(e^{j\omega\Upsilon(a)} - 1 \right)} e^{-j 2\rho_{\text{RR}} \omega \int_{\Upsilon(0)}^{\Upsilon(a)} \Upsilon^{-1}(y) e^{j\omega y} dy}
\end{aligned}
$$
$$(21)$$

which, recalling the definition of $\Upsilon(r)$ in (14), simplifies to

$$
\Phi_{I_{\text{tot}}}(\omega) = e^{-j 2\rho_{\text{RR}} \omega \int_{\Upsilon(0)}^{\Upsilon(\infty)} \Upsilon^{-1}(y) e^{j\omega y} dy} . \quad (22)
$$

Equation (14) also implies that $\Upsilon^{-1}(y) = \frac{y}{P_{\text{r0}}}^{-1/\beta}$, $\Upsilon(0) \to \infty$, and $\Upsilon(\infty) = 0$; thus we can write

$$
\begin{aligned}
\Phi_{I_{\text{tot}}}(\omega) &= e^{-j 2\rho_{\text{RR}} \omega \int_{\infty}^{0} \frac{y}{P_{\text{r0}}}^{-1/\beta} e^{j\omega y} dy} \\
&= e^{j 2\rho_{\text{RR}} \omega \int_{0}^{\infty} \frac{y}{P_{\text{r0}}}^{-1/\beta} e^{j\omega y} dy} \\
&= e^{j 2\rho_{\text{RR}} \omega \int_{0}^{\infty} \frac{y}{P_{\text{r0}}}^{-1/\beta} \cos(\omega y) dy} \\
&\quad \cdot e^{-2\rho_{\text{RR}} \omega \int_{0}^{\infty} \frac{y}{P_{\text{r0}}}^{-1/\beta} \sin(\omega y) dy} \\
&= e^{-2\rho_{\text{RR}} P_{\text{r0}}^{1/\beta} \cos\left(\frac{\pi}{2\beta}\right) \Gamma\left(\frac{\beta-1}{\beta}\right) \omega |\omega|^{\frac{1-\beta}{\beta}} \text{sign}(\omega)} \\
&\quad \cdot e^{j 2\rho_{\text{RR}} P_{\text{r0}}^{1/\beta} \sin\left(\frac{\pi}{2\beta}\right) \Gamma\left(\frac{\beta-1}{\beta}\right) \omega |\omega|^{\frac{1-\beta}{\beta}}} . \quad (23)
\end{aligned}
$$

Defining

$$
K_{\text{RR}} \triangleq 2\rho_{\text{RR}} P_{\text{r0}}^{1/\beta} \Gamma\left(\frac{\beta - 1}{\beta} \right)
$$

we then obtain

$$
\Phi_{I_{\text{tot}}}(\omega) = e^{-K_{\text{RR}} |\omega|^{\frac{1}{\beta}} \left[\cos\left(\frac{\pi}{2\beta}\right) - j \sin\left(\frac{\pi}{2\beta} \text{sign}(\omega)\right) \right]} \quad (24)
$$

which can be rearranged as

$$
\begin{aligned}
\Phi_{I_{\text{tot}}}(\omega) &= e^{-K_{\text{RR}} \cos\left(\frac{\pi}{2\beta}\right) |\omega|^{\frac{1}{\beta}} \left[1 - j \frac{\sin\left(\frac{\pi}{2\beta}\right)}{\cos\left(\frac{\pi}{2\beta}\right)} \text{sign}(\omega) \right]} \\
&= e^{-\left| \left(k \cos\left(\frac{\pi}{2\beta}\right) \right)^{\beta} \cdot \omega \right|^{\frac{1}{\beta}} \left[1 - j \cdot 1 \cdot \text{sign}(\omega) \cdot \tan\left(\frac{\pi}{2\beta}\right) \right]} . \quad (25)
\end{aligned}
$$

Equation (25) corresponds to the characteristic function of a stable distribution

$$
\varphi(t; a, b, c, \mu) = e^{jt\mu - |ct|^{a} \left(1 - jb \, \text{sign}(t) \tan\left(\frac{\pi a}{2}\right) \right)} \quad (26)
$$

with variable $t = \omega$ and parameters $a = 1/\beta$, $b = 1$, $c = \left(K_{\text{RR}} \cos\left(\frac{\pi}{2\beta}\right) \right)^{\beta}$, and $\mu = 0$. This demonstrates Proposition 1.

APPENDIX B: PROOF OF LEMMA 1

In the case of $\beta = 2$, the c.f. in (25) becomes

$$
\Phi_{I_{\text{tot}}}(\omega) = e^{\left| \frac{K_{\text{RR}}^2}{2} \omega \right|^{\frac{1}{2}} (1 - j \text{sign}(\omega))} \quad (27)
$$

which corresponds to the characteristic function of a Levy distribution, with location parameter $\mu = 0$ and scale parameter $c = \frac{K_{\text{RR}}^2}{2} = 2 P_{\text{r0}} \left(\rho_{\text{RR}} \Gamma\left(1/2\right) \right)^2$. This leads to (8), thus demonstrating Lemma 1.

APPENDIX C: PROOF OF PROPOSITION 2

Let us indicate with $\mathcal{N}$ the set of all vehicles, with d_{ij} the distance between the generic nodes $i \in \mathcal{N}$ and $j \in \mathcal{N}$, with r_i the resource allocated to i, and with $\mathcal{N}_i$ the set of nodes in $\mathcal{N} - \{i\}$ that uses the same resource as i. Proposition 2 states that the average distance between nodes using the same resource, defined as

$$
\bar{d} = \frac{\sum_{i \in \mathcal{N}} \sum_{j \in \mathcal{N}_i} d_{ij}}{\sum_{i \in \mathcal{N}} |\mathcal{N}_i|} \quad (28)
$$

where $|\mathcal{A}|$ is the cardinality of the set $\mathcal{A}$, is maximized with MD. The demonstration is provided by contradiction and shows that, starting with MD, any change reduces $\bar{d}$. Let us focus on the generic node a, which is allocated to resource $r_A = (a \mod R)$. With MD, the first node on the right of a that uses the same resource as a is node $b = a + R$. If the allocation of user a is modified to any resource in $\{1, 2, ..., R\} - \{r_A\}$, there is exactly one node c such that $x_a < x_c < x_b$. Since $x_c - x_a < x_b - x_a$, the contribution to the average distance involving the first node from a on the right has decreased. Since the same reasoning leads to the same conclusion for each additional node that uses the resource r_A on the right of a and for each node that uses the resource r_A on the left of a, it is proved that any variation in the allocation of an arbitrary node reduces the average distance between the nodes using the same resource.

APPENDIX D: PROOF OF PROPOSITION 3

A. Introduction

Given a generic receiver at distance $d_{\text{sd}} > 0$ from a source i in the position x_i, the total interference to the receiver with MD is

$$
I_{\text{tot}} = \sum_{j=-\infty, j \neq i}^{\infty} \Upsilon(|x_{i+jR} - x_i - d_{\text{sd}}|) . \quad (29)
$$

We limit our attention to situations where the receiver is to the right of the transmitter, thus in position $x_i + d_{\text{sd}}$. Please observe that, given the symmetry of the scenario, the case with the receiver on the left side occurs with probability 0.5 and leads to the same probabilities, so the conclusion remains valid even removing this hypothesis.

TABLE III
VALUES OF α_1 AND α_2.

Conditions	α_1	α_2	$\mathcal{Y}_v$
Interferer at the left of the source	+1	+1	$(0, \Upsilon(d_{sd}))$
Interferer between source and receiver	-1	+1	$(\Upsilon(d_{sd}), \infty)$
Interferer at the right of the receiver	+1	-1	$(0, \infty)$

B. Statistic of the positions

As a first step, it is useful to calculate the PDF and CDF of the distance of the n-th node from the source. Given the assumption of 1-D PPP distribution of nodes, the PDF of the distance between a node and its n-th neighbor in a specific direction (i.e., left or right) can be calculated with the same approach as [41]. Denoting Δ_n the r.v. of the n-th node distance, its CCDF can be calculated as

$$\bar{F}_{\Delta_n}(\delta) = \mathbb{P}\{\text{less than } n \text{ nodes} \in [0,\delta]\}$$
$$= \sum_{k=0}^{n-1} \frac{(\rho\delta)^k}{k!} e^{-\rho\delta} = \frac{\Gamma(n, \rho\delta)}{\Gamma(n)} \quad (30)$$

and the corresponding CDF is

$$F_{\Delta_n}(\delta) = 1 - \frac{\Gamma(n, \rho\delta)}{\Gamma(n)} . \quad (31)$$

From (30) the PDF can be obtained as[5]

$$f_{\Delta_n}(\delta) = -\frac{d\bar{F}_{\Delta_n}(\delta)}{d\delta}$$
$$= -\left[-\rho e^{-\rho\delta} \sum_{k=0}^{n-1} \frac{(\rho\delta)^k}{k!} + e^{-\rho\delta} \sum_{k=1}^{n-1} \frac{k(\rho)^k(\delta)^{k-1}}{k!} \right]$$
$$= \rho e^{-\rho\delta} \left[\sum_{k=0}^{n-1} \frac{(\rho\delta)^k}{k!} + \sum_{k=0}^{n-2} \frac{(\rho\delta)^k}{k!} \right] = \rho e^{-\rho\delta} \frac{(\rho\delta)^{n-1}}{(n-1)!}$$
$$= \frac{\rho^n}{\Gamma(n)} \delta^{n-1} e^{-\rho\delta} . \quad (32)$$

Equations (30), (31) and (32) are valid for any $\delta \geq 0$.

C. Statistic of the interference from a generic node

The second step consists in calculating the distribution of the interference generated by a node in the position x_j with respect to a useful signal generated by the position x_i and a receiver located in $x_i + d_{sd}$. For this purpose, let us first define the variable $\alpha_1 = \text{sign}(x_i - x_j) \cdot \text{sign}(d - (x_j - x_i))$ (where $\text{sign}(x)$ is the sign of x), which indicates if the interferer is between the source and receiver ($\alpha_1 = -1$) or not ($\alpha_1 = 1$), and $\alpha_2 = \text{sign}(d - (x_j - x_i))$, which indicates if the interferer is to the left of the source ($\alpha_2 = +1$) or to its right ($\alpha_2 = -1$).

Recalling (14) and using the definitions of α_1 and α_2, the interference as a function of $\delta = |x_j - x_i|$ can be calculated for any $\delta > 0$ as

$$\Upsilon^{(I)}_{\alpha_1,\alpha_2}(\delta) = \Upsilon(\alpha_1\delta + \alpha_2 d_{sd}) = P_{r0}(\alpha_1\delta + \alpha_2 d_{sd})^{-\beta} \quad (33)$$

[5]The same result can be obtained from [42, eq. (21)], assuming $j = n$, $\mu/a = \rho$ and $a \to \infty$.

and its inverse results in

$$\Upsilon^{(I)^{-1}}_{\alpha_1,\alpha_2}(y) = \alpha_1 \left[\left(\frac{y}{P_{r0}}\right)^{-1/\beta} - \alpha_2 d_{sd} \right] . \quad (34)$$

Additionally, the derivative of the inverse is

$$[\Upsilon^{(I)^{-1}}_{\alpha_1,\alpha_2}(y)]' = -\frac{\alpha_1}{\beta} P_{r0}^{1/\beta} y^{-\frac{1}{\beta}-1} . \quad (35)$$

Both (34) and (35) are valid for any positive y so that $\alpha_1 \left[\left(\frac{y}{P_{r0}}\right)^{-1/\beta} - \alpha_2 d_{sd} \right] > 0$. Using $\mathcal{Y}_v$ to describe the set in which y is valid, it results: 1) $\mathcal{Y}_v = (0, \Upsilon(d_{sd}))$ when $\alpha_1 = +1$ and $\alpha_2 = +1$; 2) $\mathcal{Y}_v = (\Upsilon(d_{sd}), \infty)$ when $\alpha_1 = -1$ and $\alpha_2 = +1$; and 3) $\mathcal{Y}_v = (0, \infty)$ when $\alpha_1 = +1$ and $\alpha_2 = -1$. All possible combinations of α_1 and α_2, and the resulting $\mathcal{Y}_v$ are summarized in Table III.

Using (32), (34), (35) and the change-of-variable technique, the PDF of the interference from the n-th node can be calculated as in the following equation, where the dependence on α_1 and α_2 is explicit.

$$f_{I_{n,\alpha_1,\alpha_2}}(y) = -f_{\Delta_n}(\Upsilon^{(I)^{-1}}_{\alpha_1,\alpha_2}(y)) \cdot [\Upsilon^{(I)^{-1}}_{\alpha_1,\alpha_2}(y)]'$$
$$= -\frac{\rho^n}{\Gamma(n)} \left(\Upsilon^{(I)^{-1}}_{\alpha_1,\alpha_2}(y)\right)^{n-1} e^{-\rho\Upsilon^{(I)^{-1}}_{\alpha_1,\alpha_2}(y)} [\Upsilon^{(I)^{-1}}_{\alpha_1,\alpha_2}(y)]'$$
$$= -\frac{\rho^n}{\Gamma(n)} \left(\alpha_1 \left(\frac{y}{P_{r0}}\right)^{-1/\beta} - \alpha_2 d_{sd} \right)^{n-1}$$
$$\cdot e^{-\rho\left(\alpha_1\left(\frac{y}{P_{r0}}\right)^{-1/\beta} - \alpha_2 d_{sd}\right)} \left(-\frac{\alpha_1}{\beta}\right) P_{r0}^{1/\beta} y^{-\frac{\beta+1}{\beta}} . \quad (36)$$

Thus, defining

$$\xi_{\alpha_1,\alpha_2}(a,b) \triangleq \alpha_1 \left(\frac{a}{P_{r0}}\right)^{-\frac{1}{\beta}} - \alpha_2 b$$

and

$$\xi'_{\alpha_1}(a) \triangleq \frac{d\xi_{\alpha_1,\alpha_2}(a,b)}{da} = \left(-\frac{\alpha_1}{\beta}\right) P_{r0}^{1/\beta} a^{-\frac{1+\beta}{\beta}}$$

we get

$$f_{I_{n,\alpha_1,\alpha_2}}(y) = \begin{cases} -\frac{\rho^n}{\Gamma(n)} (\xi_{\alpha_1,\alpha_2}(y,d_{sd}))^{n-1} \\ \quad \cdot \xi'_{\alpha_1}(y) e^{-\rho(\xi_{\alpha_1,\alpha_2}(y,d_{sd}))} & y \in \mathcal{Y}_v \\ 0 & \text{otherwise} \end{cases} \quad (37)$$

From (37), we can also write the corresponding CDF as

$$F_{I_{n,\alpha_1,\alpha_2}}(y) = \int_0^y f_{I_{n,\alpha_1,\alpha_2}}(z) dz$$
$$= \begin{cases} \frac{\Gamma(n, \rho(\xi_{\alpha_1,\alpha_2}(y,d_{sd})))}{\Gamma(R)} & y \in \mathcal{Y}_v \\ 0 & y < \min\{\mathcal{Y}_v\} \\ 1 & y > \max\{\mathcal{Y}_v\} \end{cases} \quad (38)$$

(a) Example of case 1.

(b) Example of case 2.

○ Source   ● Receiver   ⬤ Considered interferers   ⊜ Neglected interferers

(c) Legend.
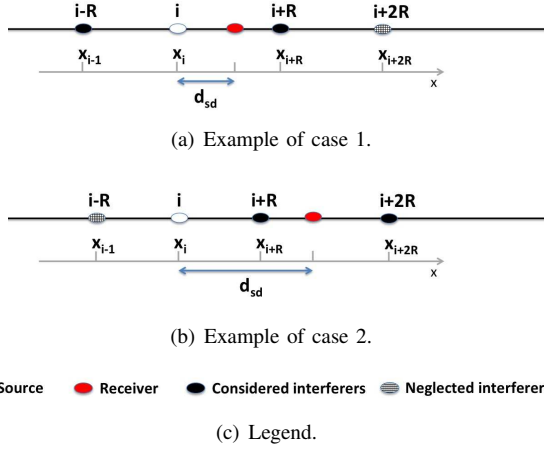
Fig. 7. MD: examples of case 1 and case 2.

D. Statistic of the overall interference

Given these premises, we can now proceed to calculate the distribution of the overall interference. For this purpose, please recall that all potential interferers are the $k \cdot R$-th farthest nodes to the right and left of the source, with k being any positive integer. If we neglect the interference from all the nodes except the interferers closest to the receiver from both directions, hereafter called left and right interferers, we can rewrite (29) as

$$I_{\text{tot}} \simeq \Upsilon(\delta^{(l)}) + \Upsilon(\delta^{(r)}) \tag{39}$$

where the values of $\delta^{(l)}$ and $\delta^{(r)}$ depend on the position of the receiver with respect to the source and to the interferers. In particular, let us neglect the case in which $d_{\text{sd}} \geq x_{i+2R} - x_i$[6] and separate the two following cases, exemplified in Fig. 7:

- Case 1: $d_{\text{sd}} < x_{i+R} - x_i$, which means that the receiver is between the source and the first interferer to the left of the source (Fig. 7(a)); this case occurs with probability $\bar{F}_{\Delta_R}(d_{\text{sd}})$ (given in (30));
- Case 2: $x_{i+R} - x_i \leq d_{\text{sd}} < x_{i+2R} - x_i$, which means that the receiver is between the first interferer to the right and the second interferer to the right of the source (Fig. 7(b)); this case occurs with probability $F_{\Delta_R}(d_{\text{sd}})$.

In the following, we first obtain the distribution of the left and right interference and then derive the CDF of I_{tot}.

Using (37) and (38), the interference caused by the first interferer to the left and to the right of the receiver for both Case 1 and Case 2 can be calculated as follows.

Left interferer. In Case 1, the interferer to the left of the receiver is node $i - R$, whereas in Case 2 it is node $i + R$. Thus, applying the law of total probability and using (37), it is

$$f_{I^{(l)}}(y) = \bar{F}_{\Delta_R}(d_{\text{sd}})f_{I_{R,+1,+1}}(y) + F_{\Delta_R}(d_{\text{sd}})f_{I_{R,-1,+1}}(y) \tag{40}$$

---

[6]The case in which $d_{\text{sd}} \geq x_{i+2R} - x_i$ occurs with probability $F_{\Delta_{2R}}(d_{\text{sd}})$; from (30), if we assume for example $R = 100$, $\rho = 0.1$, and $d_{\text{sd}} = 500$ m, it is less than 10^{-9}.

and the corresponding CDF is

$$F_{I^{(l)}}(y) = \bar{F}_{\Delta_R}(d_{\text{sd}})F_{I_{R,+1,+1}}(y) + F_{\Delta_R}(d_{\text{sd}})F_{I_{R,-1,+1}}(y) . \tag{41}$$

Right interferer. Similarly, the interferer to the left of the receiver is node $i + R$, whereas in Case 2 it is node $i + 2R$, thus it is

$$f_{I^{(r)}}(y) = \bar{F}_{\Delta_R}(d_{\text{sd}})f_{I_{R,+1,-1}}(y) + F_{\Delta_R}(d_{\text{sd}})f_{I_{2R,+1,-1}}(y) . \tag{42}$$

Statistic of the sum. Finally, given the CDF of the interference $F_{I^{(l)}}(y)$ received from the first interferer to the left in (41) and the PDF of the interference $f_{I^{(r)}}(y)$ received from the first interferer to the right in (42), and assuming that the two distributions are independent of each other,[7] the CDF of the sum interference can be written as

$$
\begin{aligned}
F_{I_{\text{tot}}}(y) &= \int_{-\infty}^{\infty} F_{I^{(l)}}(y-z)f_{I^{(r)}}(z)dz \\
&= \int_0^y \left[\bar{F}_{\Delta_R}(d_{\text{sd}})F_{I_{R,+1,+1}}(y-z) + F_{\Delta_R}(d_{\text{sd}})F_{I_{R,-1,+1}}(y-z) \right] \cdot \\
&\quad \left[\bar{F}_{\Delta_R}(d_{\text{sd}})f_{I_{R,+1,-1}}(z) + F_{\Delta_R}(d_{\text{sd}})f_{I_{2R,+1,-1}}(z) \right] dz \\
&= \left(\bar{F}_{\Delta_R}(d_{\text{sd}}) \right)^2 \int_0^y F_{I_{R,+1,+1}}(y-z)f_{I_{R,+1,-1}}(z)dz \\
&\quad + \bar{F}_{\Delta_R}(d_{\text{sd}})F_{\Delta_R}(d_{\text{sd}}) \int_0^y F_{I_{R,+1,+1}}(y-z)f_{I_{2R,+1,-1}}(z)dz \\
&\quad + \bar{F}_{\Delta_R}(d_{\text{sd}})F_{\Delta_R}(d_{\text{sd}}) \int_0^y F_{I_{R,-1,+1}}(y-z)f_{I_{R,+1,-1}}(z)dz \\
&\quad + \left(F_{\Delta_R}(d_{\text{sd}}) \right)^2 \int_0^y F_{I_{R,-1,+1}}(y-z)f_{I_{2R,+1,-1}}(z)dz \tag{43}
\end{aligned}
$$

In most cases of interest, it is $F_{\Delta_R}(d_{\text{sd}}) << 1$ (i.e., the probability that there is an interferer between source and destination is negligible), which also implies $\bar{F}_{\Delta_R}(d_{\text{sd}}) \simeq 1$; under this hypothesis and recalling (38), it follows

$$
\begin{aligned}
F_{I_{\text{tot}}}(y) &\approx \left(\bar{F}_{\Delta_R}(d_{\text{sd}}) \right)^2 \int_0^y F_{I_{R,+1,+1}}(y-z)f_{I_{R,+1,-1}}(z)dz \\
&= 1 \cdot \left[\int_0^{\min(y,\Upsilon(d_{\text{sd}}))} \frac{\Gamma\left(R, \rho\left(\xi_{R,+1,+1}\left(y-z, d_{\text{sd}}\right)\right)\right)}{\Gamma(R)} \right. \\
&\quad \left. \cdot f_{I_{R,+1,-1}}(z)dz + \int_{\min(y,\Upsilon(d_{\text{sd}}))}^y 1 \cdot f_{I_{R,+1,-1}}(z)dz \right] .
\end{aligned} \tag{44}
$$

Furthermore, in practical cases it is normally $y < \Upsilon(d_{\text{sd}})$, i.e., the useful received power is greater than the minimum acceptable interference. Thus, exploiting (37), we can write

$$
\begin{aligned}
F_{I_{\text{tot}}}(y) &\approx \int_0^y \frac{\Gamma\left(R, \rho\left(\xi_{R,+1,+1}\left(y-z, d_{\text{sd}}\right)\right)\right)}{\Gamma(R)} \\
&\quad \cdot \left(-\frac{\rho^R}{\Gamma(R)} \right) \left(\xi_{R,+1,-1}\left(z, d_{\text{sd}}\right) \right)^{R-1} \\
&\quad \cdot \xi'_{R,+1}(z)e^{-\rho(\xi_{R,+1,-1}(z,d_{\text{sd}}))}dz .
\end{aligned} \tag{45}
$$

Finally, defining $K_{\text{MD}} \triangleq -\frac{\rho^R}{(\Gamma(R))^2}$, $\xi(a,b) \triangleq \xi_{R,+1,-1}(a,b)$ (which also implies $\xi(a,b) = \xi_{R,+1,+1}(a,-b)$), and $\xi'(a) \triangleq \xi'_{R,+1}(a)$, (45) can be rearranged as in (11).

---

[7]This assumption is strictly true for Case 1 and an approximation for Case 2.

Please remark that (11) holds under the assumptions that the probability that there is an interferer between source and destination is negligible and that the useful received power is greater than the minimum acceptable interference. In the rare case that they are not valid, the solution is provided by (43).

REFERENCES

[1] "Intelligent transport systems (ITS); vehicular communications; basic set of applications; part 2: Specification of cooperative awareness basic service," *3GPP EN 302.637-2 V1.3.1*, September 2014.

[2] "DSRC message communication minimum performance requirements: Basic safety message for vehicle safety applications. draft std. j2945.1 revision 2.2, SAE," SAE, 2011.

[3] H. Seo, K. D. Lee, S. Yasukawa, Y. Peng, and P. Sartori, "LTE evolution for vehicle-to-everything services," *IEEE Communications Magazine*, vol. 54, no. 6, pp. 22–28, June 2016.

[4] S. h. Sun, J. l. Hu, Y. Peng, X. m. Pan, L. Zhao, and J. y. Fang, "Support for vehicle-to-everything services based on LTE," *IEEE Wireless Communications*, vol. 23, no. 3, pp. 4–8, June 2016.

[5] A. Bazzi, B. M. Masini, A. Zanella, and I. Thibault, "On the performance of IEEE 802.11p and LTE-V2V for the cooperative awareness of connected vehicles," *IEEE Transactions on Vehicular Technology*, vol. 66, no. 11, pp. 10 419–10 432, November 2017.

[6] S. Zhang, Y. Hou, X. Xu, and X. Tao, "Resource allocation in D2D-based V2V communication for maximizing the number of concurrent transmissions," in *IEEE 27th Annual International Symposium on Personal, Indoor, and Mobile Radio Communications (PIMRC)*, 2016, pp. 1–6.

[7] L. F. Abanto-leon, A. Koppelaar, and S. Heemstra de Groot, "Parallel and successive resource allocation for V2V communications in overlapping clusters," in *IEEE Vehicular Networking Conference (VNC)*, 2017.

[8] G. Cecchini, A. Bazzi, B. M. Masini, and A. Zanella, "Localization-based resource selection schemes for network-controlled LTE-V2V," in *International Symposium on Wireless Communication Systems (ISWCS)*, August 2017, pp. 396–401.

[9] L. Hu, J. Eichinger, M. Dillinger, M. Botsov, and D. Gozalvez, "Unified device-to-device communications for low-latency and high reliable vehicle-to-X services," in *IEEE 83rd Vehicular Technology Conference (VTC Spring)*, May 2016, pp. 1–7.

[10] R. Molina-Masegosa and J. Gozalvez, "LTE-V for sidelink 5G V2X vehicular communications: A new 5G technology for short-range vehicle-to-everything communications," *IEEE Vehicular Technology Magazine*, vol. 12, no. 4, pp. 30–39, December 2017.

[11] J. Yang, B. Pelletier, and B. Champagne, "Enhanced autonomous resource selection for LTE-based V2V communication," in *2016 IEEE Vehicular Networking Conference (VNC)*, December 2016.

[12] J. Kim, J. Lee, S. Moon, and I. Hwang, "A position-based resource allocation scheme for V2V communication," *Wireless Personal Communications*, vol. 98, no. 1, pp. 1569–1586, January 2018.

[13] G. Cecchini, A. Bazzi, B. M. Masini, and A. Zanella, "MAP-RP: Map-based resource reselection procedure for autonomous LTE-V2V," in *IEEE 28th Annual International Symposium on Personal, Indoor, and Mobile Radio Communications (PIMRC)*, 2017.

[14] J. He, Z. Tang, Z. Fan, and J. Zhang, "Enhanced collision avoidance for distributed LTE vehicle to vehicle broadcast communications," *IEEE Communications Letters*, vol. PP, no. 99, pp. 1–1, 2018.

[15] G. Cecchini, A. Bazzi, B. M. Masini, and A. Zanella, "LTEV2Vsim: An LTE-V2V simulator for the investigation of resource allocation for cooperative awareness," in *5th IEEE International Conference on Models and Technologies for Intelligent Transportation Systems (MT-ITS)*, June 2017, pp. 80–85.

[16] C. Sommer, R. German, and F. Dressler, "Bidirectionally coupled network and road traffic simulation for improved IVC analysis," *IEEE Transactions on Mobile Computing*, vol. 10, no. 1, pp. 3–15, January 2011.

[17] A. Bazzi, B. M. Masini, and A. Zanella, "How many vehicles in the LTE-V2V awareness range with half or full duplex radios?" in *15th edition of International Conference on Intelligent Transport Systems (ITS) Telecommunications (ITST)*, 2017.

[18] "Technical specification group radio access network; evolved universal terrestrial radio access (E-UTRA); physical layer procedures," *3GPP TS 36.213 V13.2.0*, June 2016.

[19] "Technical specification group radio access network; evolved universal terrestrial radio access (E-UTRA); medium access control (MAC) protocol specification," *3GPP TS 36.321 V14.4.0*, September 2017.

[20] W. Min, M. Winbjork, Z. Zhang, R. Blasco, H. Do, S. Sorrentino, M. Belleschi, and Y. Zang, "Comparison of LTE and DSRC-based connectivity for intelligent transportation systems," in *IEEE 85th Vehicular Technology Conference (VTC Spring)*, 2017.

[21] T. V. Nguyen, P. Shailesh, B. Sudhir, G. Kapil, L. Jiang, Z. Wu, D. Malladi, and J. Li, "A comparison of cellular vehicle-to-everything and dedicated short range communication," in *IEEE Vehicular Networking Conference (VNC)*, 2017.

[22] X. Cheng, L. Yang, and X. Shen, "D2D for intelligent transportation systems: A feasibility study," *IEEE Transactions on Intelligent Transportation Systems*, vol. 16, no. 4, pp. 1784–1793, August 2015.

[23] W. Sun, E. G. Strom, F. Brannstrom, K. C. Sou, and Y. Sui, "Radio resource management for D2D-based V2V communication," *IEEE Transactions on Vehicular Technology*, vol. 65, no. 8, pp. 6636–6650, August 2016.

[24] S. C. Hung, X. Zhang, A. Festag, K. C. Chen, and G. Fettweis, "An efficient radio resource re-allocation scheme for delay guaranteed vehicle-to-vehicle network," in *IEEE 84th Vehicular Technology Conference (VTC-Fall) 2016*, Sept, pp. 1–6.

[25] X. Chen, H. H. Refai, and X. Ma, "A quantitative approach to evaluate DSRC highway inter-vehicle safety communication," in *IEEE GLOBECOM 2007 - IEEE Global Telecommunications Conference*, Nov 2007, pp. 151–155.

[26] W. Zhang, Y. Chen, Y. Yang, X. Wang, Y. Zhang, X. Hong, and G. Mao, "Multi-hop connectivity probability in infrastructure-based vehicular networks," *Selected Areas in Communications, IEEE Journal on*, vol. 30, no. 4, pp. 740–747, May 2012.

[27] M. I. Hassan, H. L. Vu, and T. Sakurai, "Performance analysis of the IEEE 802.11 MAC protocol for DSRC safety applications," *IEEE Transactions on Vehicular Technology*, vol. 60, no. 8, pp. 3882–3896, October 2011.

[28] F. J. Martin-Vega, B. Soret, M. C. Aguayo-Torres, I. Z. Kovacs, and G. Gomez, "Geolocation-based access for vehicular communications: Analysis and optimization via stochastic geometry," *IEEE Transactions on Vehicular Technology*, vol. 67, no. 4, pp. 3069–3084, April 2018.

[29] "Intelligent transport systems (ITS); vehicular communications; basic set of applications; definitions," *ETSI TR 102.638 V1.1.1*, June 2009.

[30] B. M. Masini, A. Bazzi, and A. Zanella, "A survey on the roadmap to mandate on board connectivity and enable V2V-based vehicular sensor networks," *Sensors*, vol. 18, no. 7, 2018. [Online]. Available: http://www.mdpi.com/1424-8220/18/7/2207

[31] J. Kingman, *Poisson Processes*. Oxford Univ. Press, 1993.

[32] E. Salbaroli and A. Zanella, "Interference analysis in a Poisson field of nodes of finite area," *IEEE Transactions on Vehicular Technology*, vol. 58, no. 4, pp. 1776–1783, May 2009.

[33] M. Haenggi and R. K. Ganti, "Interference in large wireless networks," *Foundations and Trends in Networking*, vol. 3, no. 2, pp. 127–248, 2009.

[34] J. P. Nolan, "Numerical calculation of stable densities and distribution functions," *Communications in Statistics. Stochastic Models*, vol. 13, no. 4, pp. 759–774, 1997.

[35] "Technical specification group radio access network; study on LTE-based V2X services," *3GPP TR 36.885 V14.0.0*, July 2016.

[36] "D5.3: WINNER+ final channel models," *Wireless World Initiative New Radio – WINNER+*, June 2010.

[37] "Technical specification group radio access network; evolved universal terrestrial radio access (E-UTRA); user equipment (UE) radio transmission and reception," *3GPP TS 36.101 V15.0.0*.

[38] B. Toghi, M. Saifuddin, H. Nourkhiz Mahjoub, M. O. Mughal, Y. P. Fallah, J. Rao, and S. Das, "Multiple Access in Cellular V2X: Performance Analysis in Highly Congested Vehicular Networks," in *Vehicular Networking Conference (VNC), 2018 IEEE*, December.

[39] A. Bazzi, G. Cecchini, A. Zanella, and B. M. Masini, "Study of the impact of PHY and MAC parameters in 3GPP C-V2V mode 4," *IEEE Access*, pp. 1–1, 2018.

[40] A. Bazzi, B. M. Masini, A. Zanella, and A. Calisti, "Visible light communications as a complementary technology for the internet of vehicles," *Elsevier Computer Communications, Special issue on Multiradio, Multi-technology, Multi-system Vehicular Communications*, 2016.

[41] M. Haenggi, "On distances in uniformly random networks," *IEEE Transactions on Information Theory*, vol. 51, no. 10, pp. 3584–3586, October 2005.

[42] A. Zanella, A. Bazzi, G. Pasolini, and B. M. Masini, "On the impact of routing strategies on the interference of ad hoc wireless networks," *IEEE Transactions on Communications*, vol. 61, no. 10, pp. 4322–4333, October 2013.

Alessandro Bazzi (S'03-M'06-SM'18) received the Laurea degree and the Ph.D. degree in telecommunications engineering both from the University of Bologna, Italy, in 2002 and 2006, respectively. Since 2002, he works with the Institute of Electronics, Computer and Telecommunication Engineering (IEIIT) of the National Research Council of Italy (CNR) and since the academic year 2006/2007, he has been acting as adjunct Professor at the University of Bologna. His work mainly focuses on connected vehicles and heterogeneous wireless access networks, with particular emphasis on medium access control, routing and radio resource management. Dr. Bazzi serves as a Reviewer and TPC Member for various international journals and conferences and he is currently in the Editorial Board of Hindawi's Mobile Information Systems and Wireless Communications and Mobile Computing.

Barbara M. Masini (S'02-M'05) received the Laurea degree (summa cum laude) in Telecommunications Engineering and the Ph.D. degree in Electronic, Computer Science, and Telecommunication engineering from the University of Bologna, Italy, in 2001 and 2005, respectively. Since 2005, she is a researcher at the Institute for Electronics and for Information and Telecommunications Engineering (IEIIT), of the National Research Council (CNR). Since 2006 she is also adjunct Professor at the University of Bologna. She works in the area of wireless communication systems and her research interests are mainly focused on connected vehicles, from physical and MAC levels aspects up to applications and field trial implementations. Research is also focused on relay assisted communications, energy harvesting, and visible light communication (VLC). She is Editor of Elsevier Computer Communication, Guest Editor of Elsevier Ad Hoc Networks, Special Issue on Vehicular Networks for Mobile Crowd Sensing (2015), Mobile Information Systems, Special Issue on Connected Vehicles: Applications and Communication Challenges (2017), Sensors, Special Issue on Sensors Networks for Smart Roads (2018). She is Secretary of Chapter VT06/COM19 of the IEEE Italy section. She is TPC member of several conferences, reviewer for most international journals and for the Italian Ministry of Economic Development (MISE).

Alberto Zanella (S'99-M'00-SM'12) received the Laurea degree (summa cum laude) in Elecronic Engineering from the University of Ferrara, Italy, in 1996, and the Ph.D. degree in Electronic Engineering and Computer Science from the University of Bologna in 2000. In 2001 he joined the CNR-CSITE (merged in CNR-IEIIT since 2002) as a researcher and, since 2006, as senior researcher. His research interests include MIMO, mobile radio systems, ad hoc and sensor networks, vehicular networks. Since 2001 he has the appointment of Adjunt Professor of Electrical Communication (2001 - 2005), Telecommunication Systems (2002-2012-2013), Multimedia Communication Systems (2006 - 2011) at the University of Bologna. He participated/participate to several national and European projects. He was Technical Co-Chair of the PHY track of the IEEE conference WCNC 2009 and of the Wireless Communications Symposium (WCS) of IEEE Globecom 2009. He was/is in the Technical Program Committee of several internation conferences, such as ICC, Globecom, WCNC, PIMRC, VTC. He had served as Editor for Wireless Systems (2003-2012), IEEE Transactions on Communications and he is currently Senior Editor for the same journal.

Giammarco Cecchini (S'17) received the Laurea degree (summa cum laude) in Telecommunications Engineering in Bologna in 2016, awarded with a prize from Lions Club Fondazione Guglielmo Marconi for his master thesis entitled "Performance of LTE-V2V for Cooperative Awareness". Since 2017, he joined the Institute of Electronics, Computer and Telecommunication Engineering (IEIIT) of the National Research Council of Italy (CNR). His work mainly focuses on wireless technologies for connected vehicles, both including IEEE 802.11p (with related standards) and LTE-V2X. He is also the main developer of the open-source MATLAB simulator LTEV2Vsim.